

1 Measuring the Impact of Cushion Design on Buttocks Tissue

2 Deformation: An MRI Approach

3

4 Abstract

5 Aim: To establish a research approach for describing how different wheelchair cushion designs impact
6 buttocks tissue deformation during sitting.

7 Materials and Methods: The buttocks of 4 individuals with spinal cord injury and significant atrophy
8 were scanned sitting in a FONAR Upright MRI. Scans were collected with the individuals' buttocks fully
9 suspended without pelvic support, and seated on 3 different commercially available wheelchair
10 cushions. Multi-planar scans were analyzed to provide 3D renderings and measurements of tissue
11 thickness and shape.

12 Results: Bulk tissue thicknesses at the ischium, which rarely included muscle, were reduced by more
13 than 60% on enveloping cushion designs studied (i.e., Roho HP and Matrx Vi), and more variably (23-
14 60%) on an orthotic off-loading design (i.e., Java). Adipose was typically displaced posterior and superior
15 from the unloaded condition, with more lateral displacement on the Roho HP and Matrx Vi and more
16 medial displacement present on the Java. Large changes in angle at the sacro-coccygeal joint indicated
17 significant loading on the region. Deformation at the greater trochanter was more consistent across
18 surfaces. Greater interface pressures tended to be associated with greater deformation, but the
19 relationship varied by individuals and was highly non-linear.

20 Conclusions: The buttocks in this study all deformed significantly, but at different locations and in
21 different manners across all 3 surfaces. Attention needs to be paid to the regions of greatest

22 deformation. A future metric of shape compliance should consider cushion performance at all high risk
23 regions, and changes to the amount and shape of tissue in the regions of interest.

24 Keywords

25 Pressure Ulcer, Wheelchair cushion, MRI, buttocks, multi-planar, tissue deformation

26

27 Background

28 Individuals who use wheelchairs are at high risk of developing pressure ulcers due to their reduced
29 mobility and sensation. Consequently, pressure ulcers negatively impact health, activities of daily living,
30 employment, and quality of life of wheelchair users (1-4). Individuals with a pressure ulcer are at
31 increased risk for future pressure ulcer development (5) and premature death (2, 5).

32 Although there are many contributing factors to pressure ulcer development, tissue deformation is
33 implicated in all physiological pathways including direct deformation damage, as well as ischemia
34 secondary to deformation of blood vessels and impaired lymphatic drainage (6-10). Individuals who
35 experience more tissue deformation when seated are considered to have a high Biomechanical Risk for
36 pressure ulcer development. In distinction, deformation resistance is defined as “the intrinsic
37 characteristic of an individual’s soft tissues to withstand extrinsic applied forces.” (11) (12). Pressure
38 ulcer prevention therefore seeks to reduce tissue deformation.

39 Skin protection wheelchair cushions are frequently prescribed for wheelchair users considered at
40 risk for pressure ulcers (13). Skin protection cushions require that cushions meet a minimum level (40
41 mm) of immersion using a standardized test (14, 15). That standard is met by a variety of approaches
42 that manage body weight very differently in terms of design, materials and construction. Two common

43 approaches to managing body weight include envelopment and offloading. With an enveloping design,
44 the buttocks immerse into the wheelchair cushion and the cushion envelops the tissue to increase
45 contact area and minimize pressure gradients. An offloading cushion will redistribute body mass away
46 from particular bony prominences, ideally to tissue better suited to withstand the load (16). One metric
47 of cushion performance that can be used across designs of wheelchair cushions is shape compliance.
48 Shape Compliance describes the ability of a cushion to support the buttocks with minimal buttocks
49 deformation.

50 Recent studies have moved beyond interface pressure as the primary metric of cushion
51 performance, and have begun to consider internal responses using a compliant buttocks model (16) and
52 human participants (17, 18). The studies of humans have been focused on the amount of tissue present
53 underneath the peak of the ischial tuberosity (17, 18). However, these studies miss two important
54 issues. First, they do not explain how the cushions work, only how much tissue is displaced away from
55 the ischium. Second, they do not consider tissue loading and deformation at the other high risk areas for
56 seated pressure ulcers: the sacrum and greater trochanters.

57 Therefore, the primary objective of this study was to utilize a case series to establish a research
58 approach for describing how different wheelchair cushion designs impact buttocks tissue deformation
59 during sitting.

60 Methods

61 Participants

62 For this case series, we selectively targeted four participants at high risk for pressure ulcer development.
63 They were full-time wheelchair users with complete spinal cord injuries and significant atrophy who
64 represented some of the more challenging active individuals to safely seat. Participants needed to sit

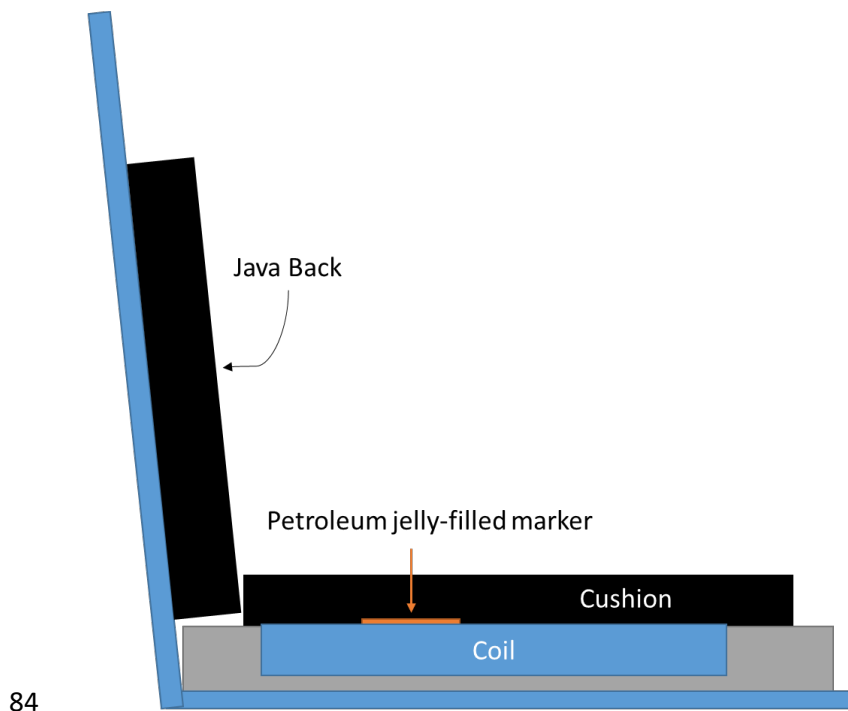
65 with a level and neutral pelvic posture, and be able to sit safely on the cushions under investigation for
66 15 minutes each. Participants were excluded if they had a current pressure ulcer, could not maintain a
67 stable upright posture on the cushions being studied, or had any condition that contraindicated safe
68 participation in MRI scans. Institutional Review Board approval was received from the local institution
69 and informed consent was acquired from the recruited subjects.

70

71 MRI Test Environment

72 Subjects wore loose fitting clothing to the study. Subjects were scanned in an upright unloaded posture,
73 and seated on 3 commercially available wheelchair cushions. These cushions were: an orthotic
74 offloading cushion (Java, Ride Designs), a pressure redistribution cushion made with contoured foam
75 (Matrx Vi, Invacare), and a pressure redistribution cushion that uses air flotation (Roho HP, Permobil). In
76 the unloaded condition, the participants maintained a seated posture, and body weight was supported
77 under the thighs and through a thoracic suspension support, thereby offloading the ischium, greater
78 trochanters, coccyx and lower sacrum.

79 The scan environment included a flat, rigid seat base including the MRI coil, topped with a petroleum
80 jelly-filled platform surface marker, and the wheelchair cushion or thigh support for the unloaded
81 condition (Figure 1). The seat to back angle was 96° and a Java seat back insert with integrated
82 abdominal support (Ride Designs) was adhered to a rigid seat back to provide trunk suspension in the
83 unloaded condition and improve balance on the three cushion test conditions.



84

85 *Figure 1. Illustration of test environment*

86 MRI Study Protocol

87 For loaded cushions, a random order was used and determined prior to the scan session. The cushions
88 were then placed in the scanner on top of the coil and marker (Figure 1). Subjects were seated on the
89 cushion in compliance with each cushion manufacturer's instructions for use. An effort was made to
90 align their pelvis in a neutral posture. The footrest was adjusted to properly load the thighs and to keep
91 the knees and hips close to 90 degrees of flexion and ensure consistent thigh support in each test
92 condition.

93 Subjects seated on the Roho cushion were palpated to confirm inflation of the cushion in accordance
94 with the manufacturer's recommendations. A range of 0.5-1" of air between the user's bottom and the
95 seating surface was targeted. An MRI scout image containing 5 slices near the ischial tuberosity was
96 collected to permit measurement from the cushion base (identified by the platform surface marker) to
97 the skin below the ischium, and adjustments were made to the cushion inflation as appropriate.

98 Subjects seated on the Java cushion were palpated to confirm that the ischium were offloaded. The
99 subjects were also palpated to confirm that their greater trochanters rested in relief on the sides of the
100 cushion. Subjects were centered on the Matrix Vi, but no further adjustments were performed. When
101 possible, the tissue was briefly unloaded after palpating via a weight shift.

102 *Imaging Protocol*

103 The scans were collected using a RF-spoiled Gradient Recalled Echo protocol, with 80 contiguous sagittal
104 slices of 3 mm thickness which provided a coverage of 240 mm. The effective slice thickness was 3.8 mm
105 due to under sampling in the slice-encoding direction, which was done to save time. An in-plane
106 resolution of 1.5 mm was acquired in both the frequency- and phase-encoding directions. The total scan
107 time was 8 minutes and 24 seconds.

108

109 *Data Processing*

110 Raw DICOM scans were imported into AnalyzePro (AnalyzeDirect, Overland Park, KS) for review and
111 segmentation of the pelvis, femur, gluteus maximus, and subcutaneous fat. Segmentation was
112 performed under the supervision of an experienced radiographer (BLINDED FOR REVIEW). Skin was
113 included within the subcutaneous fat segmentation when visible, since the scan resolution did not allow
114 for separate segmentation of the two. Point clouds of the 3D segmented surfaces of the bones, muscle,
115 and fat were exported for further analysis in Matlab R2016 (MathWorks, Natick, MA). The peak of the
116 ischial tuberosity and the most inferior point of the greater trochanter when seated were manually
117 identified by a trained student (BLINDED FOR REVIEW) and a radiographer (BLINDED FOR REVIEW), and
118 consensus was reached with regards to the locations.

119 *Data Analysis*

120 Muscle volume was reported from AnalyzePro based on the manually segmented gluteus maximus and,
121 consistent with previous work, the percent gluteus coverage was defined as the percent of a cylindrical
122 50 mm region under the peak of the ischial tuberosity covered by more than 2 mm of gluteus maximus
123 (12).

124 The amount of tissue present inferior to the bony prominences, or the average Bulk Tissue Thickness,
125 was defined to include skin, connective tissue, adipose, and muscle (when present). Bulk Tissue
126 Thickness under the ischium was measured in an oblique plane in a region 50mm long. The oblique
127 plane was defined as the plane running through the ischium in a posterior-lateral orientation, such that
128 the 50mm region of interest included predominantly tissue beneath bone, rather than tissue
129 surrounding the bone (Figure 2). More specifically, an axial slice 15 mm superior to the peak of the
130 ischium was selected. In that plane, a line was drawn connecting the most medial anterior point and the
131 most lateral, posterior point of the ischium. The oblique plane was defined to run through this line and
132 perpendicular to the axial plane. This Bulk Tissue Thickness was highly correlated with the fat and
133 gluteus maximus tissue thicknesses reported on in (12) but was easier to calculate. Tissue deformation
134 was defined as the normalized change in bulk tissue thickness compared with unloaded.

135
$$Deformation = \frac{Thickness_{Unloaded} - Thickness_{Cushion}}{Thickness_{Unloaded}} * 100$$

136 We also calculated the radius of curvature of the superficial skin surface within a cylindrical 50 mm
137 region of interest centered on the ischium in the sagittal and coronal planes (12).

138 Greater trochanter bulk tissue thickness was calculated in a 50 mm cylindrical region of interest under
139 the most inferior point of the greater trochanter (Figure 2). Similar to measurements calculated at the
140 ischium, this included skin, connective tissue, adipose and muscle.

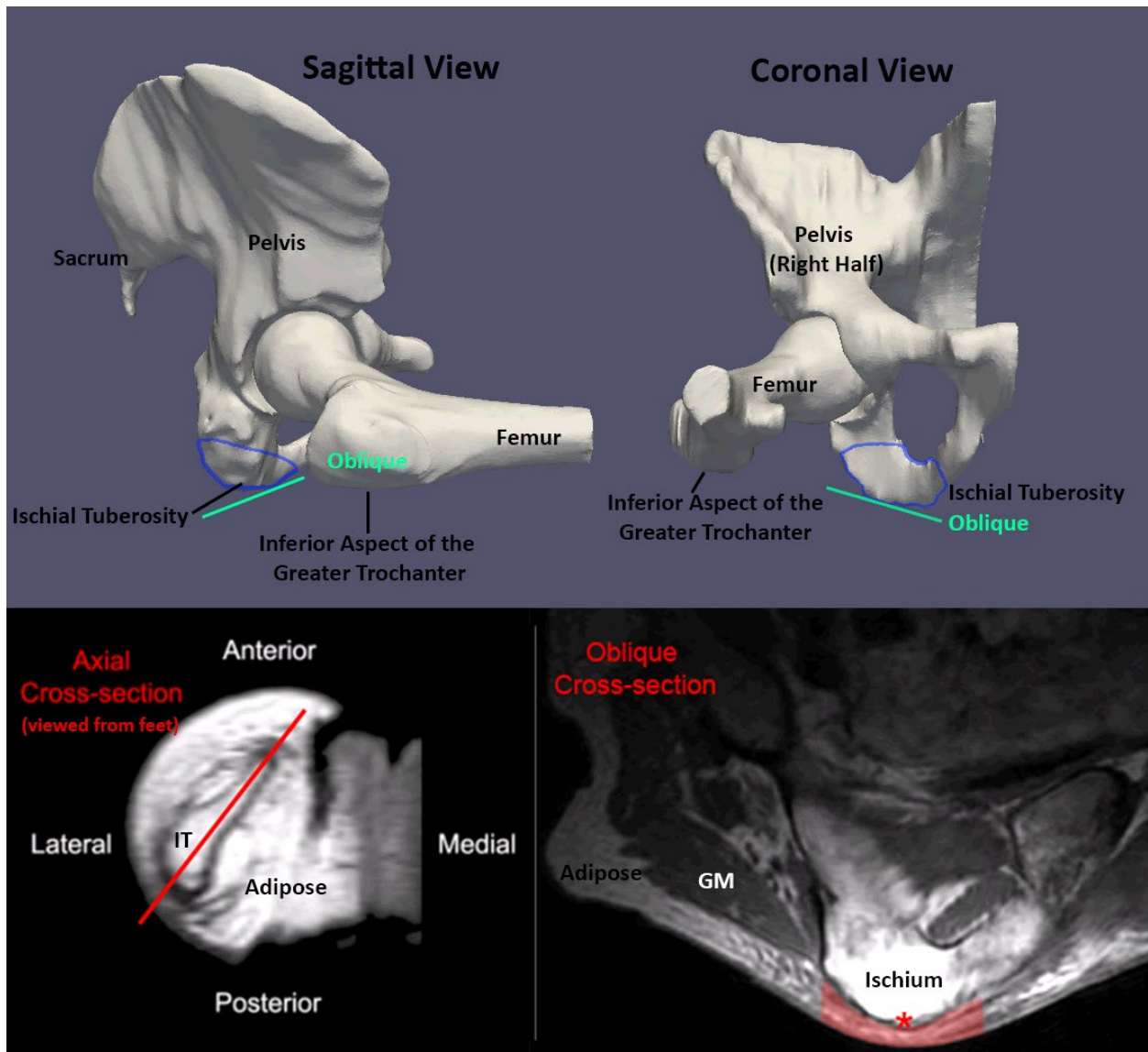
141 Finally, changes in the sacro-coccygeal angle were measured, as loads applied at the coccyx will rotate
142 this mobile joint, reducing the sacro-coccygeal angle. The angle was defined as the angle between the
143 line drawn from the midpoint of the upper edge of the S1 vertebra and the midpoint of the upper edge
144 of the coccyx (Cx1) vertebra, and the line drawn from the midpoint of the upper edge of the coccyx (Cx1)
145 vertebra with the distal aspect of the coccyx Cx3 vertebra according to (19) (Figure 3).

146 [Interface Pressure Mapping Protocol](#)

147 Interface pressure mapping (IPM) was done in the same seated posture, but in a wheelchair with seating
148 configured to match that of the MRI, specifically a complete Java back and a rigid seat pan, with a 96
149 degree seat to back angle and horizontal seat pan orientation as in the MRI platform. Participants
150 transferred onto the wheelchair cushion (studied in the same order that cushions were scanned in the
151 MRI) with an FSA Boditrak (Vista Medical) mat on top of the cushion. Ischial tuberosities (ITs) were
152 palpated to locate the ITs on the FSA mat and then participants performed a depression lift to relieve
153 pressure on their buttocks. Participants sat for 2 minutes and then data was collected at 0.2 Hz for 30
154 seconds. Peak pressure index (20) was calculated under both ischium and averaged across all frames.

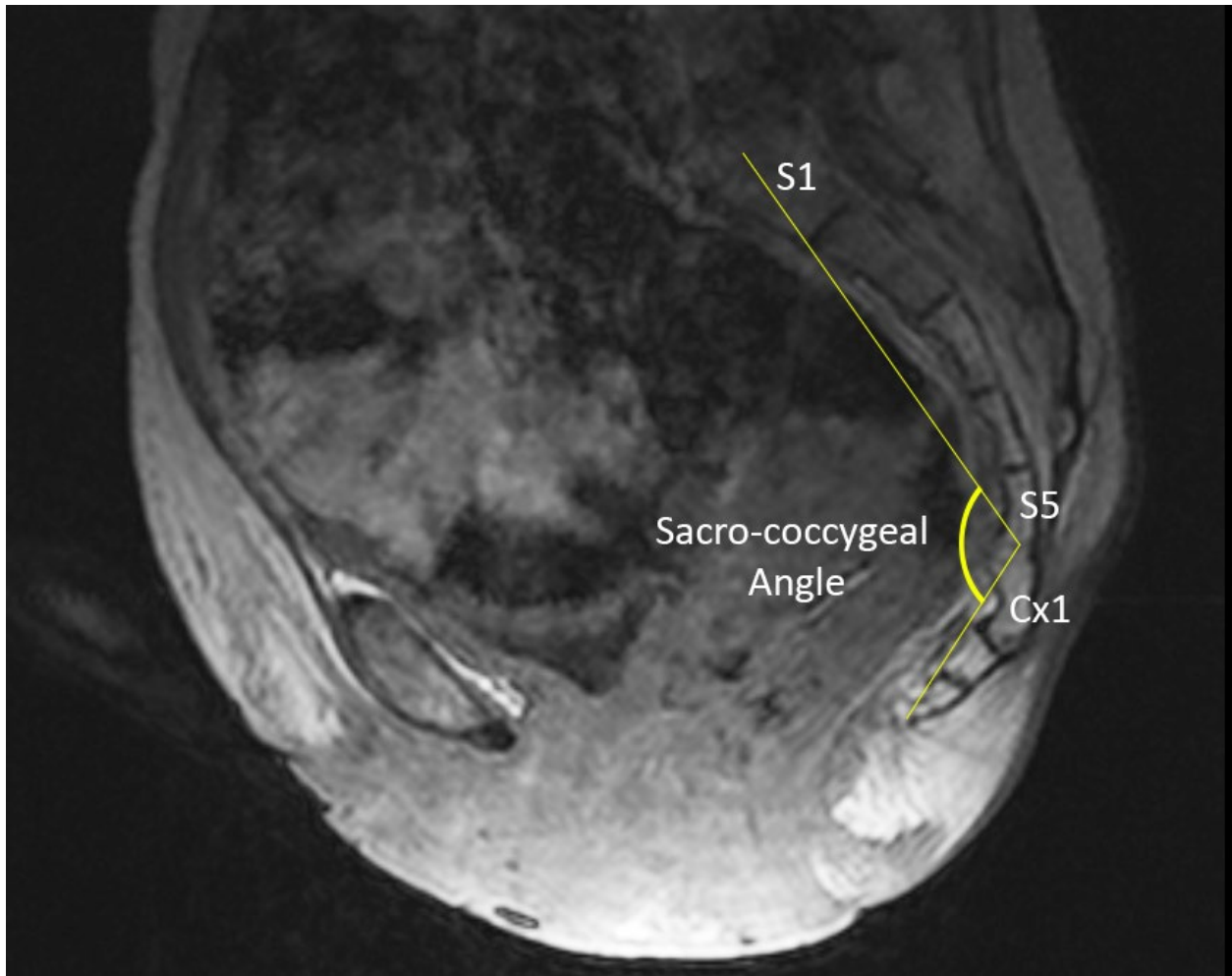
155

156



157

158 *Figure 2. Identification of relevant bony anatomy. Sagittal and coronal views of a rendering of the right half of the pelvis and*
 159 *proximal femur are shown with the inferior aspect of the greater trochanter marked, as well as the oblique orientation of the*
 160 *ischium. The axial cross section of the MRI (bottom left) illustrates the oblique plane that runs through the posterior-lateral*
 161 *orientation of the ischial tuberosity (IT). Peak of the ischial tuberosity (*) marked on the oblique cross-section, and bulk tissue*
 162 *included in the calculation of average thickness is highlighted in red (bottom right). Adipose and gluteus maximus (GM) are also*
 163 *identified in the image.*



164

165 *Figure 3. Sacro-coccygeal angle was defined as the angle between the line drawn from the midpoint of the upper edge of the S1*
166 *vertebra and the midpoint of the upper edge of the coccyx (Cx1) vertebra, and the line drawn from the midpoint of the upper*
167 *edge of the coccyx (Cx1) vertebra with the distal aspect of the coccyx Cx3 vertebra.*

168 **Results**

169

170 **Study Participants**

171 Four participants with complete spinal cord injuries (Table 1) were included in this study.

Subject ID	Gender	Age	Weight (lbs)	Level of SCI	Years Post Injury	Pri Status
A	F	32	95	T11	5	None
B	M	44	163	T5-6	18	Recurrent (Ipsilateral)
C	F	46	124	T12	24	None
D	F	46	130	T2-4	16	Right after injury

172

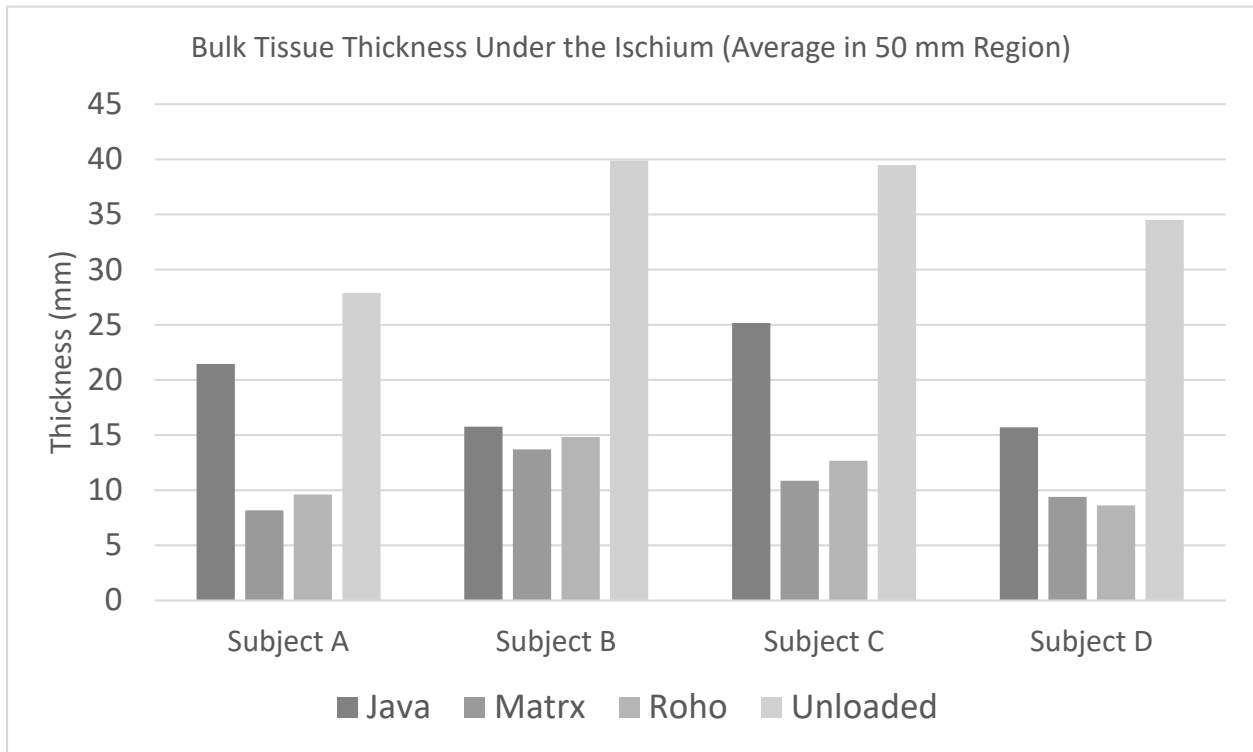
173 **Buttocks Anatomy**

174 The buttocks anatomy was consistent across the four participants in that each presented with significant
175 muscle atrophy (Muscle volume average: 265 cm³ and range: 171 to 447 cm³) and limited soft tissue at
176 the ischium (Bulk tissue thickness range: 28-40 mm, Figure 4). In one participant (C), we were unable to
177 assess muscle characteristics because the fatty infiltration was so significant that it was not possible to
178 determine where adipose tissue ended and muscle began.

179 Previous studies have raised the question of where the gluteus maximus is located during sitting. In this
180 cohort of participants, gluteus maximus wrapped posterior and lateral to the ischium, with < 17% of the
181 ischium covered by gluteus maximus across all unloaded and loaded conditions. This is evident in Figure
182 5 by noticing the ischium (white) visible below the red gluteus maximus.

183

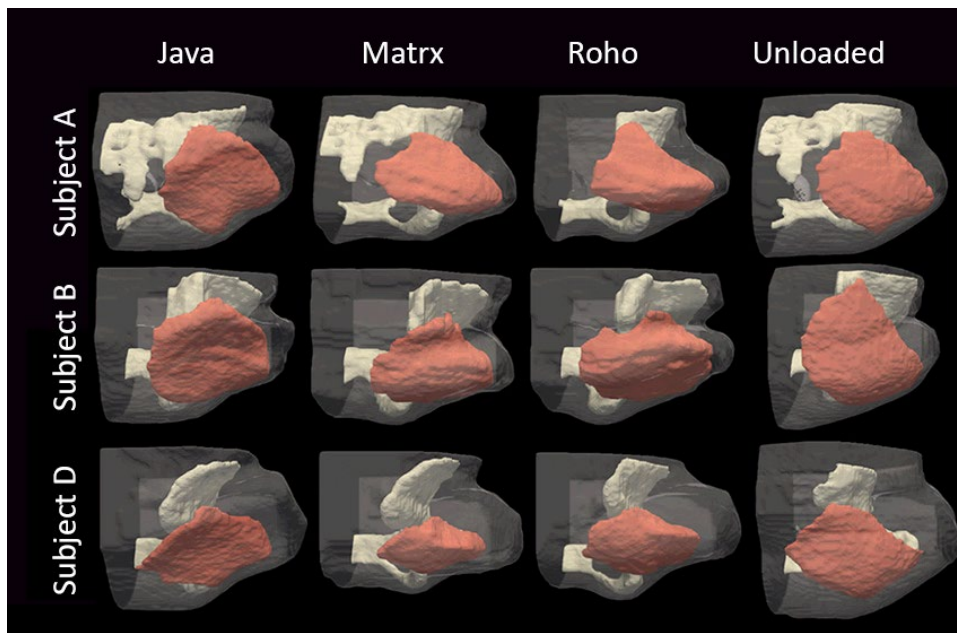
184



185

186

Figure 4. Bulk tissue thickness under the ischium varied across cushions., but were fairly similar across subjects.



187

188 *Figure 5. 3D renderings of the right half of the buttocks pictured from the posterior present the skin as semi-transparent so that*
189 *the pelvis (white) and gluteus maximus (red) are visible. Note that the sacrum is not included or is only partially included in these*
190 *images*

191 Quantitative description of cushion loading

192 Bulk Tissue Deformation under the IT

193 Reduction in bulk tissue thicknesses when seated on the Matrx Vi and Roho HP as compared with
194 unloaded thicknesses was greater than 60% (Figure 4). Bulk tissue thicknesses on these surfaces were
195 fairly similar and small across subjects. More variation in tissue thicknesses and deformation was
196 evident across cushions, with thicknesses on the Java being considerably larger than on the Roho HP and
197 Matrx Vi for 3 of 4 participants. Subject B, however, had a similar bulk tissue thickness and deformation
198 under the ischium on all 3 cushions.

199
200 When tissue thickness was reduced under load, it did so via displacement rather than compression.
201 Typically, adipose was displaced posterior and superior from the unloaded condition, although the
202 precise displacement varied by individual and especially by cushion. More lateral displacement was
203 evident on the Roho HP and Matrx Vi, while there was more medial displacement on the Java.

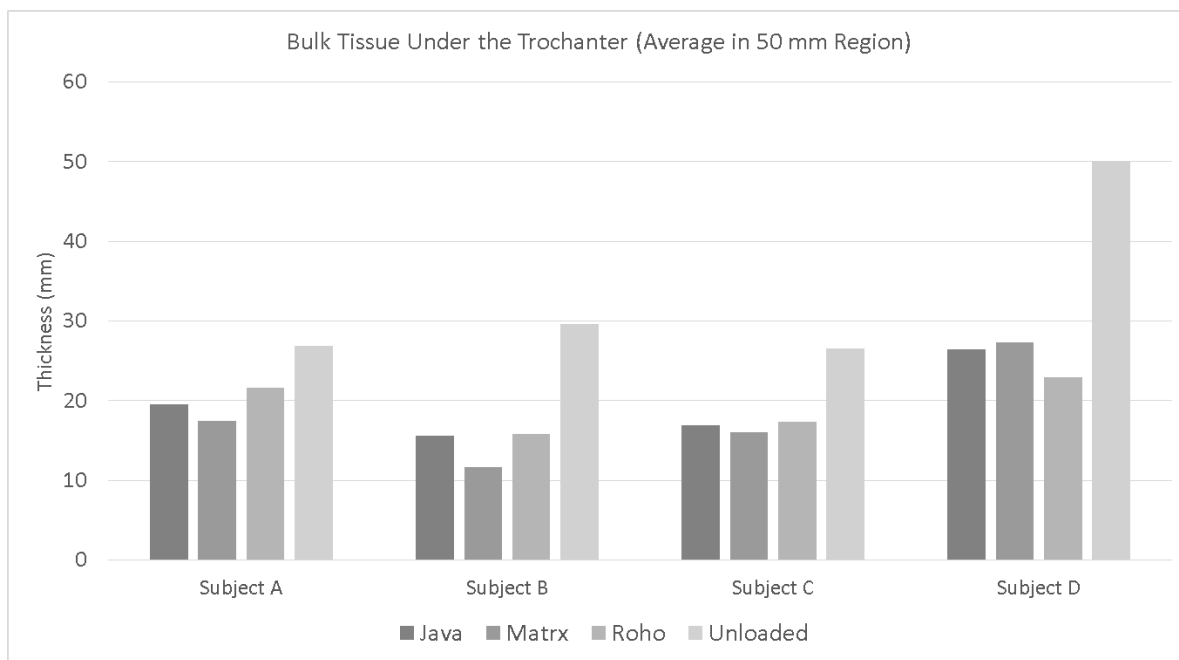
204

205

206 Bulk Tissue Deformation under the Trochanter

207 Bulk tissue thickness under the greater trochanter was relatively consistent across subjects and cushions
208 (Figure 6). Tissue thickness under the trochanter, which included gluteus maximus as well as adipose,
209 connective tissue, and skin, ranged from 12-27mm in the loaded condition, or deformation from
210 unloaded of 19-61%. Subject B displayed the largest tissue deformations beneath the trochanter relative

211 to unloaded (61%). Adipose and gluteus maximus present under the trochanter in the unloaded
212 condition displaced laterally under load.
213

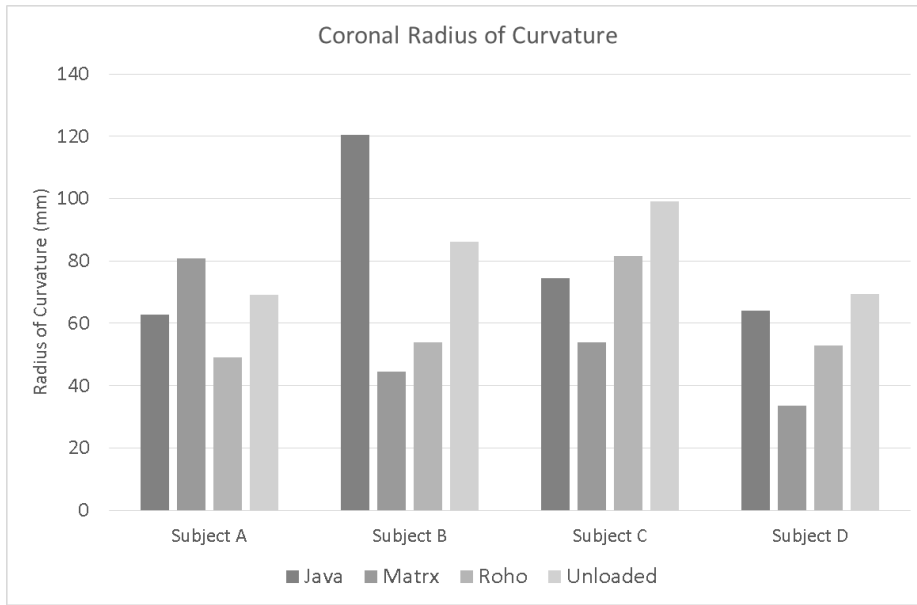


214
215 *Figure 6. Bulk tissue under the greater trochanter was similar across cushions.*

216 Radius of Curvature of Superficial Tissue under the IT

217 In most cases, the buttocks experienced the greatest radius of curvature, or flattest surface contour, in
218 the unloaded condition (Figure 7, Figure 8, Figure 9). In the sagittal plane, the tissue with the smallest
219 radius of curvature, or most pointed surface was seen when seated on the Matrx Vi and Roho HP, with
220 similar curvatures across the surfaces. The sagittal curvature was typically greater on the Java than
221 Matrx Vi and Roho HP, but the magnitude of that difference varied across subjects. Curvatures in the
222 coronal plane differed more across cushions. The high radius of curvature on the Java for Subject B is
223 indicative of the skin making contact with the bottom surface of the cushion well, creating an essentially
224 flat shape.

225

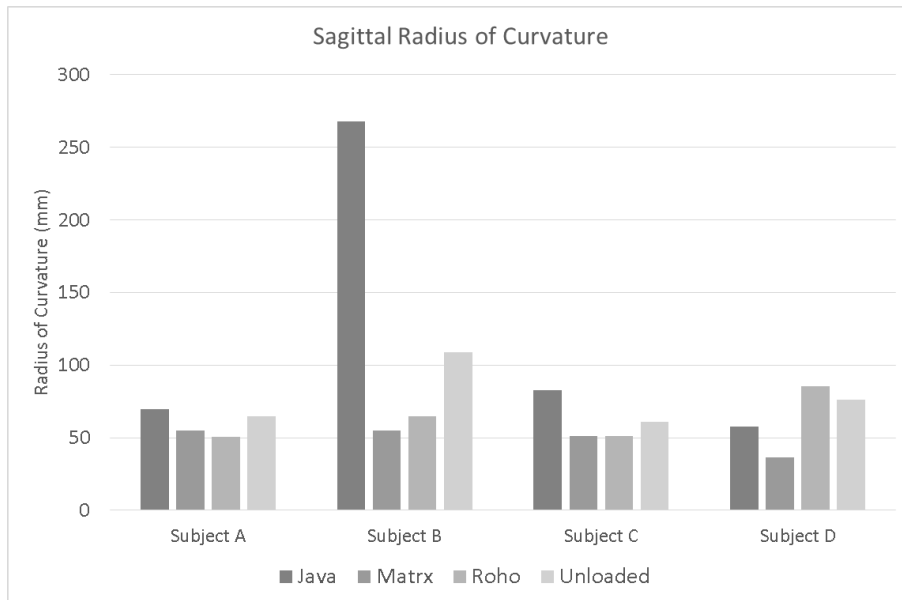


226

227

Figure 7. Radius of curvature of the skin beneath the ischium in the coronal plane.

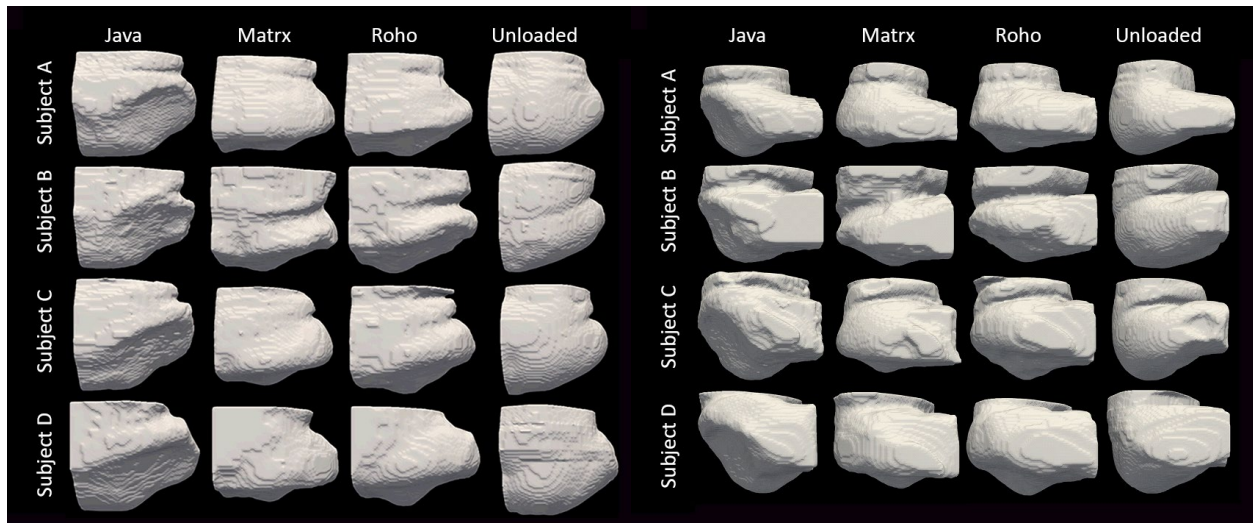
228



229

230

Figure 8. Radius of curvature of the skin beneath the ischium in the sagittal plane.



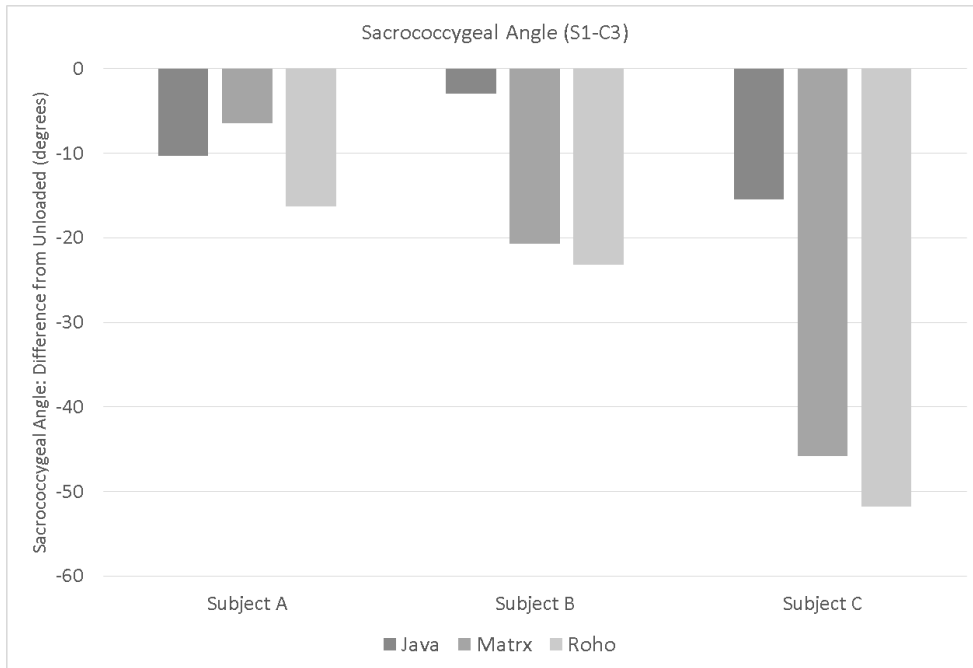
231

232 *Figure 9. 3D Renderings of skin from the right half of the buttocks pictured from the lateral coronal view (Left) and posterior*
 233 *(Right). Note that flat edges in the lateral view depict the end of our field of view (e.g., Subject I on Java) and do not reflect the*
 234 *actual shape of the lateral tissue.*

235

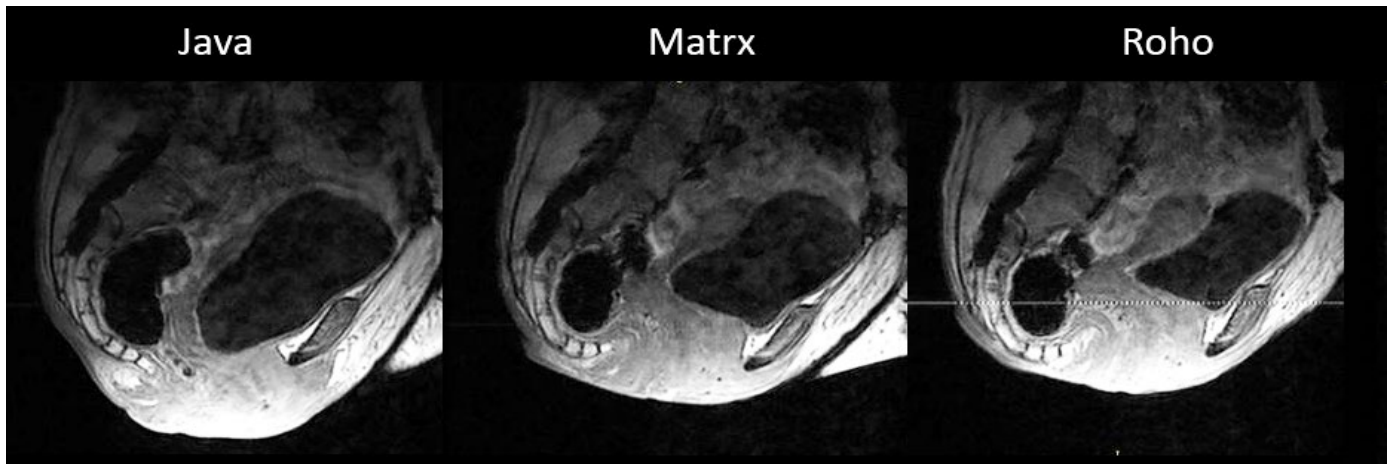
236 **Sacral Loading**

237 S1 was only visible in 3 participants because an artifact interfered with the image at the level of S1 in the
 238 fourth, so sacro-coccygeal angle was only reported for these 3 participants. When sitting in a loaded
 239 condition, the angle between the sacrum and coccyx was reduced on all cushions, but angle changes
 240 were greatest on the Roho HP. This is illustrated for Subject B in Figure 11.



241

242 *Figure 10. Change in Sacro-coccygeal angle compared with unloaded.*



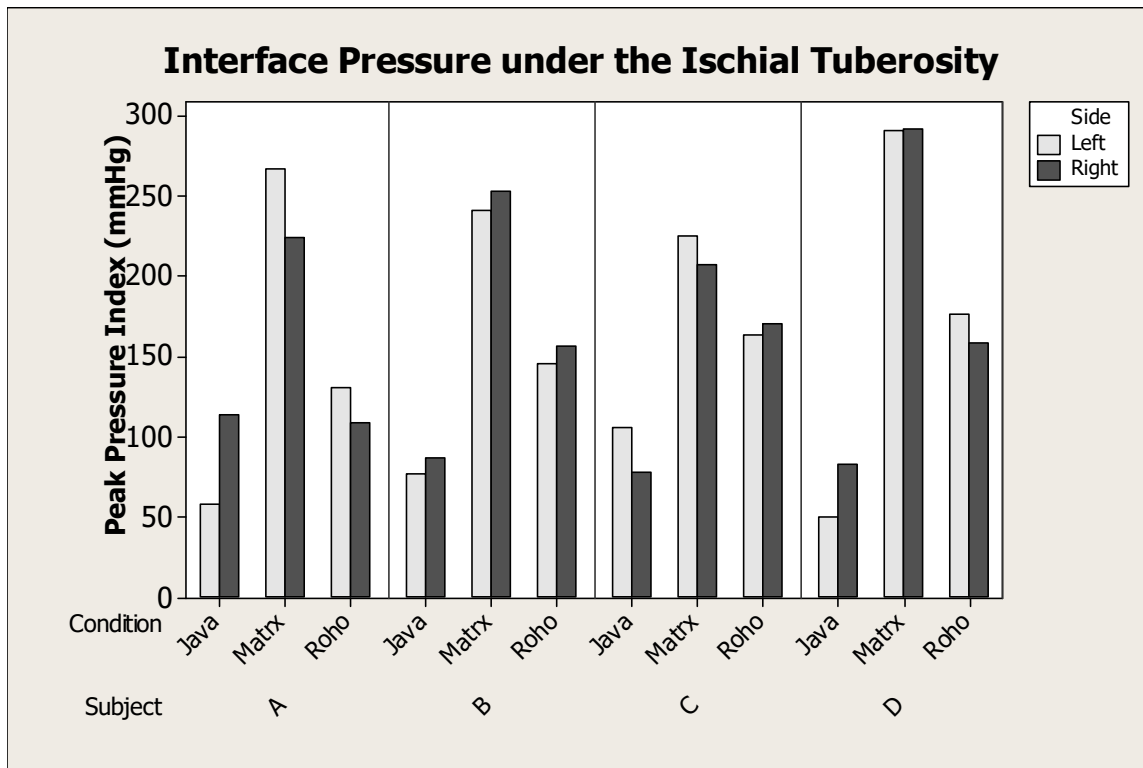
243

244 *Figure 11. Mid-sacrum coronal slices for Subject B demonstrate the differences in coccyx orientation during sitting on different*
 245 *surfaces.*

246 **Interface Pressure Results**

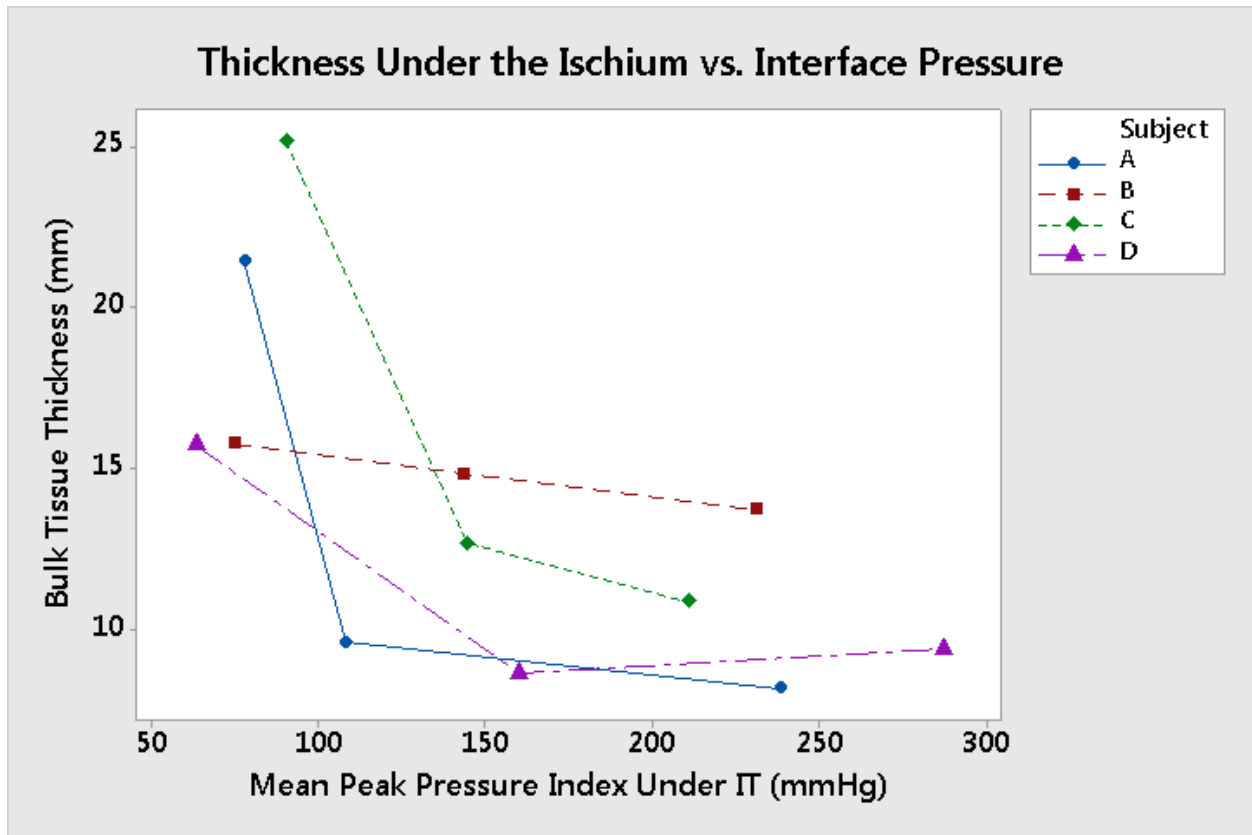
247 Peak Pressure Indices (PPIs) varied from 50 to 290 mmHg, with the lowest PPIs experienced while
 248 participants were seated on the Java, and the greatest on the Matrix Vi (Figure 12). While higher

249 pressures often corresponded with increased deformation, that pattern was not always the case within
250 nor across individuals (Figure 13).



251

252 *Figure 12. Interface pressure measured under the ischial tuberosities.*



254

255 *Figure 13. Relationship between tissue deformation and interface pressure under the ischium.*

256 Overall Mechanisms of Support Across Cushions

257

258 The unloaded and loaded buttocks tissue obtained a different shape on each loading condition, as visible
259 in the sagittal and coronal views presented in Figure 9.

260

261 Roho HP

262 The Roho cushion is an example of an air cell design, in which air redistributes between a matrix of
263 connected cells in response to buttocks loading, resulting in envelopment of the buttocks. This design
264 seeks to increase contact area and minimize pressure gradients. Cushions with similar designs include
265 the Standard Contour Cushion by Star Cushion and the Pressure Equalization Pad by Ongoing Care
266 Solutions, Inc.

267 Immersion of the buttocks into the Roho HP, or deflection of the Roho HP under load, was set by the
268 investigators by adjusting the inflation level of the cushion. However, final measurements of the
269 distance from the most inferior point of the buttocks to the seat base varied from 1.7 to 3.0 cm,
270 corresponding to immersion values of 7.8-9.1 cm. The corresponding envelopment is visible in Figure 9,
271 where the discontinuity in the surface contour represents the edge of envelopment. The inferior
272 adipose and skin wrapped around the peak of the ischium, as evident by the decreased radius of
273 curvature compared with unloaded (Figure 7 and Figure 8). Bulk tissue beneath the ischium changed in
274 thickness by 2-2.5 cm compared with unloaded, displacing in the superior, posterior and lateral
275 directions. Surrounding tissue was loaded from all directions around the ischium. Similarly, tissue
276 around the greater trochanter was loaded at an angle for most participants. While the gluteus maximus
277 did not wrap beneath the ischium during unloaded sitting, it displaced in the superior and lateral

278 directions when seated on the Roho HP (Figure 5). This is shown in Figure 5 as the red gluteus maximus
279 being visible to the right and above the peak of the ischial tuberosity.

280 [Matrx Vi](#)

281 The Matrx Vi is a contoured foam cushion that uses multiple layers of different foam stiffnesses,
282 including a viscoelastic layer, that seeks to envelop the buttocks and distribute loading based on
283 compression of the foam layers. Many different manufacturers distribute contoured foam cushions with
284 differing contours and material selections. The Comfort Acta-Embrace is an example of a similar cushion.

285 Because the Matrx Vi is a contoured cushion, less deflection of the cushion is expected for an equivalent
286 amount of buttocks immersion compared with a flat cushion. Consistent with that, deflection of the
287 Matrx under load was much smaller than on the Roho, with values ranging from 2.8-4.3 cm.

288 Envelopment is visible in Figure 9. Similar to the Roho, the ischium sinks into the cushion, resulting in
289 soft tissue wrapping closely around the ischium, with decreased radius of curvatures compared with
290 unloaded. Unlike the Roho HP, however, loading seems to be mostly vertical, with the tissue posterior
291 and anterior to the ischial region taking on a flat shape. The greater trochanter was loaded by a flat
292 surface for most participants. Compared to the unloaded condition, the gluteus maximus compressed
293 and deformed superiorly and laterally, and as in the other conditions, was not loaded by the ischium.

294 [Java](#)

295 The Java is designed to support load differently than immersion and envelopment based cushions such
296 as the Roho HP and Matrx Vi. Instead, the Java takes an orthotic approach, using a balance of loading
297 and off-loading characteristics. Consequently, the shape of the deformed buttocks looks different than
298 on the Roho HP and Matrx Vi, with a large flat segment of skin and soft tissue in the gluteal region
299 where the posterior-lateral supporting component of the Java cushion supports and deforms the tissue
300 immediately inferior to the posterior iliac crest (Figure 9). Deformation is also noted at the posterior

301 proximal thigh just distal to the greater trochanters. In addition to supporting load at the posterior-
302 lateral region and at the proximal thigh, tissue deformation beneath the greater trochanter suggests
303 support of body weight there as well, in similar amounts to the other cushions. Despite complete
304 offloading in 3 of 4 participants, tissue under the ischium still experiences deformation, with 23-60%
305 deformation of bulk thickness. Adipose tends to displace in postero-medial and superior directions.
306 Radius of curvatures tend to be greater (flatter) when seated on the Java compared with enveloping
307 cushions. When seated on the Java, participants' gluteus maximus was deformed forward or anterior to
308 cover a greater portion of the inferior-posterior portion of the ischium (Figure 5). Consequently, the
309 presentation of the gluteus maximus was most similar to that of the unloaded buttocks when seated on
310 the Java, but for most participants, even on the Java the gluteus maximus was still not loaded by the
311 ischium.

312

313 Discussion

314 Comparison to Previous Work

315 As the scope of previous research regarding seated buttocks tissue deformation continues to grow,
316 some consistent findings are noted. Foremost is the lack of muscle under the ischium, observed as little
317 to no gluteus maximus present under the peak of the ischial tuberosity (12, 17, 18). This finding
318 continues to suggest that finite element models depicting considerable muscle coverage are not
319 consistent with actual anatomy (21, 22).

320 Bulk tissue deformation has been observed in the approximate range of 30-70% in people with spinal
321 cord injuries across previous studies (17) (18). These results are fairly consistent with the current study,
322 as was the variation noted across participants and surfaces. Based on these findings, the goal of ongoing

323 and future work must be to determine clinical characteristics of participants that will help in predicting
324 the individual's response to sitting on different cushions.

325 Interface pressure mapping is a clinical tool used to evaluate clients as they sit upon one or more
326 cushions. In 2007, Gefen and Levine published an article on why using interface pressure was a poor
327 choice (23) and in 2009 Oomens, et. al also wrote about the importance of internal strain over interface
328 pressure (24). We believe that IPM has clinical utility during seating evaluations. IPM can be used to
329 identify cushions that poorly redistribute pressure, as indicted by high pressure magnitudes or
330 asymmetry. The results of the present study and prior work corroborate that opinion. Results reflected a
331 nonlinear relationship between interface pressure and tissue thickness which differed across
332 participants. Figure 13 indicates that at higher pressures, corresponding buttock tissue thicknesses are
333 smaller. This response is predicted by theoretical tissue mechanics, and illustrates that the tissues under
334 the ischium can 'bottom-out' or reach maximum deformation at different interface pressures,
335 depending on the individual. This result is similar to those found in previous studies. Sonenblum et. al,
336 found a fairly wide range of individual tissue compliance in 35 persons with spinal cord injury (25). Using
337 a tissue probe capable of measuring force and deflection, a 4.2 N force induced between 3.5 and 15.2
338 mm of tissue deflection, which represented between 64-96% of maximum deflection before the tissue
339 bottomed out. Brienza, et al (26) found a relationship between IPM and tissue stiffness using a
340 computerized support surface capable of controlling forces applies to the buttocks. In a cohort of
341 persons with SCI, the results indicated that higher pressures were associated with higher stiffness. The
342 authors inferred that greater tissue deformation resulted from the higher pressures and resulted in
343 greater tissue stiffness at those loading levels. Using MRI in a recent study, Brienza et. al (17) did not
344 find a group-wise significant relationship, and only some participants showed individual relationships
345 between IPM and deformation. Their results support the idea that stress and strain might not be tightly
346 correlated across cushion designs.

347

348 To better inform seating evaluations, the relationship between interface pressure and deformation
349 should be further investigated. Because the IPM-deformation relationship appears to vary across
350 individuals, it may be possible to use interface pressure to reflect deformation when combined with
351 other individual characteristics such as age, diagnosis, tone, hip width, tissue thickness, and tissue
352 compliance. Larger cohorts are needed that reflect a diversity of individual characteristics to establish
353 clinical guidelines for IPM.

354 [Mechanisms of Support](#)

355 Wheelchair cushions use different approaches to manage body weight and reduce tissue loading and
356 deformation at high risk areas such as the ischium, greater trochanters, and sacrum/coccyx. The Java
357 uses an orthotic offloading approach, while Matrx Vi and Roho HP use envelopment and immersion,
358 albeit in different manners. The results presented above on this cohort demonstrate that the orthotic,
359 off-loading approach of the Java successfully offloaded the ischium in 3 of 4 cases, which led to reduced
360 (but not eliminated) deformations of tissue beneath the ischium and increased deformation in the
361 posterior-lateral region of the buttocks and the proximal thighs. The contoured foam cushion (Matrx Vi)
362 allowed only a small amount of immersion in this population, leading to some redistribution of load
363 across the pelvis and thighs. The air cell design of the Roho HP seeks to create a flotation effect while
364 the individual is immersed in the air bladders. Consistent with this, the data showed loading appearing
365 to wrap around the buttocks from multiple directions where it is enveloped in the cushion.

366 How tightly the tissue wraps around the ischium is in part reflected by the radius of curvature, with
367 smaller radii beneath the ischium indicating tighter wrapping. The smallest radii of curvature were
368 typically found in the enveloping cushion designs, although the data illustrate variability across

369 individuals (Figure 7 and Figure 8). Despite this variability, Figure 9 demonstrates some consistency in
370 shape of the seated buttocks within each cushion, reflecting the cushion's shape compliance.

371 Biomechanical Risk

372 The study population was hand-picked to represent individuals with high risk buttocks that are difficult
373 to support. Between the significant muscle atrophy and hypotonicity, and changes to the tissue
374 compliance that are not documented in this study, there is not much tissue available to support the
375 ischium. As the result of the reduced tissue quantity and quality, the pelvis nearly collapses through the
376 soft tissue. Despite the lack of support for the pelvis and significant atrophy, however, only two of the
377 four participants have experienced pressure ulcers. Further investigation is warranted to explain this. It
378 is also worth exploring the possibility of deep tissue damage existing without concurrent visible changes.
379 It is important to remember that amongst individuals who qualify for a skin protection wheelchair
380 cushion, varying levels of biomechanical risk will be seen and loading conditions on the cushions
381 presented are likely to differ considerably. In fact, even amongst these 4 participants, some
382 considerable differences were noted in changes in tissue thickness, radius of curvature, and overall
383 loading.

384 Wheelchair Cushion Shape Compliance

385 Wheelchair cushion shape compliance describes the ability of a cushion to support body mass without
386 deforming the buttocks. Of course, when seated on any wheelchair cushion, the body will experience
387 some deformation. Therefore, it becomes important not only to measure deformation, but to define
388 shape compliance in a manner that considers the tissue responses across all of the high-risk regions in
389 sitting. For example, deformation of tissue under the ischium was smallest for the Java, but all three
390 cushions had comparable deformation under the greater trochanter. Similarly, tissue deformation under

391 the ischium was often greater on the Matrx Vi than the Roho HP, but the change in angle at the sacrum
392 (reflecting increased loading) was greater on the Roho HP than the Matrx Vi.

393 [Sacrum and Coccyx Loading](#)

394 This is the first study to report on the tissue response to sitting at the sacrum and coccyx. In general,
395 pressure ulcers are more prevalent at this region than at the ischium (27, 28), so the response is
396 important to investigate. Tissue deformation is difficult to assess in this region, so instead we chose to
397 look at the change in angle of the sacro-coccygeal joint. As the angle decreases and the coccyx inverts,
398 greater localized strains will be applied to the soft tissue present in the region. Figure 10 and Figure 11
399 demonstrate that the angle changes varied according to both cushion and subject. It is notable,
400 however, that participants were seated upright in a relatively neutral posture. Sacral loading and
401 deformation would likely change in a more slouched posture.

402 [Clinical Implications for seating](#)

403 Understanding the deformation of the seated buttocks in this study provides some clinical insight. First,
404 the results demonstrate that in every sitting condition there is some deformation present at the
405 ischium, but that the regions of greatest deformation tend to vary. Paying attention to those regions is
406 important. Significant loading of the sacrum and coccyx occurs, even in upright sitting.

407 The relationship between interface pressure and deformation was not linear nor consistent. However,
408 clinically speaking, interface pressures still have value. As mentioned previously, the areas of greatest
409 deformation are important and can often be identified using interface pressure mapping. Furthermore,
410 in the cases presented, most of the very high interface pressures still corresponded with higher tissue
411 deformation. While the deformation response depended on far more than interface pressure, in a
412 clinical setting, observation of relatively high peak pressures at high risk bony prominences may

413 encourage the seating professional to adjust and or pursue a more effective sitting surface, especially if
414 skin redness has been noted.

415 Finally, achieving optimal seating conditions, even with expert skills was still challenging. Roho inflation
416 was not always correct on the first try, nor was proper offloading on the Java always achieved on the
417 first try. This leads to the question of how individuals maintain appropriate adjustment and how they
418 position themselves on the cushions. Future work should investigate how cushion performance is
419 maintained over time and how it varies according to posture, particularly individuals' typical sitting
420 postures and activities, which are likely to differ from that supported in the test conditions described.
421 Cushions need to perform well in a variety of conditions.

422 [Limitations](#)

423 As a case series of only 4 individuals, this study was not designed to draw broad, generalizable
424 conclusions about cushion performance, but instead was designed to inform future studies to that end.
425 As mentioned, the cohort of individuals was limited, as all had a very similar presentation and because
426 deformation is dependent on individual characteristics, results are unlikely to generalize to individuals
427 with different body types or diagnoses. Furthermore, individuals were scanned in relatively neutral
428 postures, and as mentioned previously, cushion performance in other postures and during other
429 activities should also be investigated. The duration of loading on cushions was approximately 15-20
430 minutes, so cushions with viscoelastic or temperature sensitive properties such as the Matrx Vi may
431 deform further over time, allowing for increased immersion and possibly even bottoming out. Finally,
432 this subset of cushions was selected because they represented different strategies of managing body
433 weight. However, many cushion designs were not explored and would benefit from further study.

434 Conclusion

435 This was the first study to describe how different wheelchair cushion designs impact overall buttocks
436 tissue deformation during sitting. The results highlighted the fact that all cushions deformed tissue
437 somewhere, and that cushion design impacts how and where tissues deform. Shape compliance is a
438 construct that can be used to describe performance, but it must first be defined. Future investigation of
439 cushion designs needs to consider deformations at the ischium, coccyx, and trochanter. Parameters to
440 describe deformation at these locations should be multi-planar and represent changes to the amount
441 and shape of tissue. They may include: average thicknesses over a region of interest, radii of curvature
442 of the skin, and the sacro-coccygeal angle to describe sacral loading. Three dimensional visualizations of
443 the tissue response provide greater insight to the measurements. Finally, the results of this study
444 highlighted the importance of individual characteristics on buttocks response to load, even within
445 persons at high risk. Tools to evaluate individuals' biomechanical risk are necessary for optimizing
446 wheelchair cushion prescription.

447 Acknowledgements

448 Blinded for review

449 Funding

450 Blinded for review

451 References

- 452 1. Clark FA, Jackson JM, Scott MD, Carlson ME, Atkins MS, Uhles-Tanaka D, et al. Data-based
453 models of how pressure ulcers develop in daily-living contexts of adults with spinal cord injury. Arch
454 Phys Med Rehabil. 2006;87(11):1516-25.
- 455 2. Lala D, Dumont FS, Leblond J, Houghton PE, Noreau L. Impact of pressure ulcers on individuals
456 living with a spinal cord injury. Archives of physical medicine and rehabilitation. 2014;95(12):2312-9.

- 457 3. Langemo DK, Melland H, Hanson D, Olson B, Hunter S. The lived experience of having a pressure
458 ulcer: a qualitative analysis. *Advances in skin & wound care*. 2000;13(5):225-35.
- 459 4. Lourenco L, Blanes L, Salome GM, Ferreira LM. Quality of life and self-esteem in patients with
460 paraplegia and pressure ulcers: a controlled cross-sectional study. *Journal of wound care*.
461 2014;23(6):331-4, 6-7.
- 462 5. Guihan M, Garber SL, Bombardier CH, Goldstein B, Holmes SA, Cao L. Predictors of pressure
463 ulcer recurrence in veterans with spinal cord injury. *J Spinal Cord Med*. 2008;31(5):551-9.
- 464 6. Oomens CW, Bressers OF, Bosboom EM, Bouten CV, Blader DL. Can loaded interface
465 characteristics influence strain distributions in muscle adjacent to bony prominences? *Comput Methods*
466 *Biomech Biomed Engin*. 2003;6(3):171-80.
- 467 7. Sprigle S, Sonenblum S. Assessing evidence supporting redistribution of pressure for pressure
468 ulcer prevention: a review. *J Rehabil Res Dev*. 2011;48(3):203-13.
- 469 8. Oomens CW, Bader DL, Loerakker S, Baaijens F. Pressure induced deep tissue injury explained.
470 *Annals of biomedical engineering*. 2015;43(2):297-305.
- 471 9. Loerakker S, Manders E, Strijkers GJ, Nicolay K, Baaijens FP, Bader DL, et al. The effects of
472 deformation, ischemia, and reperfusion on the development of muscle damage during prolonged
473 loading. *Journal of applied physiology*. 2011;111(4):1168-77.
- 474 10. Stekelenburg A, Oomens CW, Strijkers GJ, Nicolay K, Bader DL. Compression-induced deep tissue
475 injury examined with magnetic resonance imaging and histology. *J Appl Physiol*. 2006;100(6):1946-54.
- 476 11. Sonenblum SE, Sprigle SH, Cathcart JM, Winder RJ. 3-dimensional buttocks response to sitting: a
477 case report. *Journal of tissue viability*. 2013;22(1):12-8.
- 478 12. Sonenblum SE, Sprigle SH, Cathcart JM, Winder RJ. 3D anatomy and deformation of the seated
479 buttocks. *J Tissue Viability*. 2015;24(2):51-61.
- 480 13. Change to Wheelchair Cushion HCPCS Codes: Noridian Healthcare Solutions; 2004 [Available
481 from: https://www.dmeprd.com/resources/articles/2004/12_14_04.html.
- 482 14. Sprigle S, Press L, Davis K. Development of uniform terminology and procedures to describe
483 wheelchair cushion characteristics. *J Rehabil Res Dev*. 2001;38(4):449-61.
- 484 15. Wheelchair Seating - Policy Article (A52505) 2017 [cited 2017. Available from:
485 <https://med.noridianmedicare.com/documents/2230703/7218263/Wheelchair+Seating+LCD+and+PA/78eccd60-ce13-40db-8127-a3aec591e176>.
- 486 16. Kumar N, Sprigle S, Martin JS. Measurement of Load Redistribution Properties of Wheelchair
487 Cushions Using a Compliant Cushion Loading Indenter. *Assist Technol*. 2015;27(3):129-35.
- 488 17. Brienza D, Vallely J, Karg P, Akins J, Gefen A. An MRI investigation of the effects of user anatomy
489 and wheelchair cushion type on tissue deformation. *Journal of tissue viability*. 2017.
- 490 18. Call E, Hetzel T, McLean C, Burton JN, Oberg C. Off loading wheelchair cushion provides best
491 case reduction in tissue deformation as indicated by MRI. *Journal of tissue viability*. 2017;26(3):172-9.
- 492 19. Tetiker H, Kosar MI, Cullu N, Canbek U, Otag I, Tastemur Y. MRI-based detailed evaluation of the
493 anatomy of the human coccyx among Turkish adults. *Niger J Clin Pract*. 2017;20(2):136-42.
- 494 20. Sprigle S, Dunlop W, Press L. Reliability of bench tests of interface pressure. *Assist Technol*.
495 2003;15(1):49-57.
- 496 21. Levy A, Kopplin K, Gefen A. An air-cell-based cushion for pressure ulcer protection remarkably
497 reduces tissue stresses in the seated buttocks with respect to foams: finite element studies. *Journal of*
498 *tissue viability*. 2014;23(1):13-23.
- 500 22. Levy A, Kopplin K, Gefen A. A Computer Modeling Study to Evaluate the Potential Effect of Air
501 Cell-based Cushions on the Tissues of Bariatric and Diabetic Patients. *Ostomy Wound Manage*.
502 2016;62(1):22-30.
- 503 23. Gefen A, Levine J. The false premise in measuring body-support interface pressures for
504 preventing serious pressure ulcers. *Journal of medical engineering & technology*. 2007;31(5):375-80.

- 505 24. Oomens CW, Loerakker S, Bader DL. The importance of internal strain as opposed to interface
506 pressure in the prevention of pressure related deep tissue injury. *Journal of tissue viability*. 2009.
- 507 25. Sonenblum SE, Sprigle SH. Buttock tissue response to loading in men with spinal cord injury.
508 *PLoS One*. 2018;13(2):e0191868.
- 509 26. Brienza DM, Karg PE. Seat cushion optimization: a comparison of interface pressure and tissue
510 stiffness characteristics for spinal cord injured and elderly patients. *Arch Phys Med Rehabil*.
511 1998;79(4):388-94.
- 512 27. Scheel-Sailer A, Wyss A, Boldt C, Post MW, Lay V. Prevalence, location, grade of pressure ulcers
513 and association with specific patient characteristics in adult spinal cord injury patients during the
514 hospital stay: a prospective cohort study. *Spinal Cord*. 2013;51(11):828-33.
- 515 28. Zhou Q, Yu T, Liu Y, Shi R, Tian S, Yang C, et al. The prevalence and specific characteristics of
516 hospitalised pressure ulcer patients: A multicentre cross-sectional study. *J Clin Nurs*. 2017.

517